NJC

Accepted Manuscript

Cobalt oxide hollow nanoparticles as synthesized by templating tri-block copolymer micelle

with core-shell-corona structure: a promising anode material for lithium ion batteries

Nhut Minh Dang[1], Wen-Wen Zhao[1], Shin-ichi Yusa[2], Hideyuki Noguchi[1], Kenichi Nakashima[1*]

[1]*Department of Chemistry, Graduate School of Science and Engineering, Saga University, 1 Honjo-machi, Saga 840-8502, Japan*

[2]*Department of Materials Science and Chemistry, University of Hyogo, 2167 Shosha, Himeji, Hyogo 671-2280, Japan*

[*]Corresponding author.
Tel.: +81 952 28 8850
Fax: +81 952 28 8548.
E-mail address: nakashik@cc.saga-u.ac.jp (K. Nakashima).

Cobalt oxide (Co_3O_4) hollow nanosphere has been fabricated by templating micelle of an anionic tri-block copolymer, poly(styrene-*block*-metharcrylic acid-*block*- ethyleneglycol) (PS-PMA-PEG), which has *core-shell-corona* structure in aqueous solutions. TEM images indicate that the inner diameter of the nanosphere is ca. 30 ± 2 nm, which is corresponding to the diameter of the PS core (ca. 30 ± 2 nm) of the template micelle. The outer diameter is about ca. 60 ± 3 nm, and the thickness of the shell is around 15 ± 1 nm, which could prevent rupture during application. The Co_3O_4 hollow nanosphere was then applied to lithium ion batteries, and showed promising electrochemical properties as anode materials (> 500 mAh.g^{-1} after 30 cycles).

Key word: cobalt oxide, hollow nanosphere, tri-block copolymer, core-shell-corona micelle, lithium battery

Introduction

Inorganic hollow nanospheres have been attracting tremendous attention of the researchers due to their unique properties such as high ratio of surface area to volume, large pore volume and low density, which provides them with potential applications in biomedical fields and electronics.[1-3] Synthesis of inorganic hollow nanospheres has been carried out by many methods. The methods can be classified into three categories: hard template method, soft template method, and template-free method. While hard template method usually gives large (micro-sized) hollow nanospheres and less yield, soft template method has several advantages: it provides smaller hollow nanospheres, tunable void size and shell thickness, as well as high yield.[4] Although the template-free method is a facile and cost-reducing method, the size of the hollow nanospheres is quite irregular.

Magnetic nanostructures with different morphology and dimensions have been produced many years ago. They include nano-sphere, nano-rod/tube/wire, nanocage,[5-8] and so on. The magnetic property depends on the size, shape and component materials. Magnetic hollow nanospheres are expected to show different physical properties in comparison with dense particles due to the confined hollow nanostructures. Cobalt oxide (Co_3O_4) is one of the most studied magnetic oxides due to its stability in alkaline media and promising potential abilities.[9,10] They have been applied in electronic devices[11], gas sensors[12], electro-chromic[13] and electrochemical systems[14]. Cobalt oxides were also used in biomedicine as the contrast enhancement agents for magnetic resonance imaging or for drug delivery.[15]

Recently, we proposed a novel technique to synthesize inorganic hollow nanospheres by using a triblock copolymer which forms *core-shell-corona* micelle.[16, 17] This method gives overall control of the structure of the nanosphere; void space of the nanosphere can be tuned by the molecular weight of the core-forming block, and the shell thickness can be adjusted by the chain length of shell-forming block and the amount of precursor. Furthermore, the corona of the polymeric micelle prevents the secondary aggregation of the nanosphere during preparation. By using the *core-shell-corona* micellar template, varieties of inorganic hollow nanosphere have been fabricated, i.e. SiO_2[18], TiO_2[19], Fe_3O_4[20], La_2O_3[21], CuO[22], ZnO[23], $ZnBO_3$[24], etc.

In the present study, we tried to synthesize hollow nanospheres of cobalt oxide (Co_3O_4) using

anionic tri-block copolymer, poly(styrene-*block*-metharcrylic acid-*block*-ethyleneglycol) (PS-PMA-PEG), as a new polymer for the template. This polymer forms a polymeric micelle with PS core, PMA shell, and PEG corona in aqueous solutions. The PS core acts as the template for the spacious void of the hollow particle, the PMA shell plays the role as the reservoir and reactor of the precursor and the PEG corona keeps the micelle-precursor composite stable in aqueous media (Scheme 1). The as-prepared cobalt oxide hollow nanospheres have an outer diameter of ca. 60 ± 3 nm and shell thickness of ca. 15 ± 1 nm.
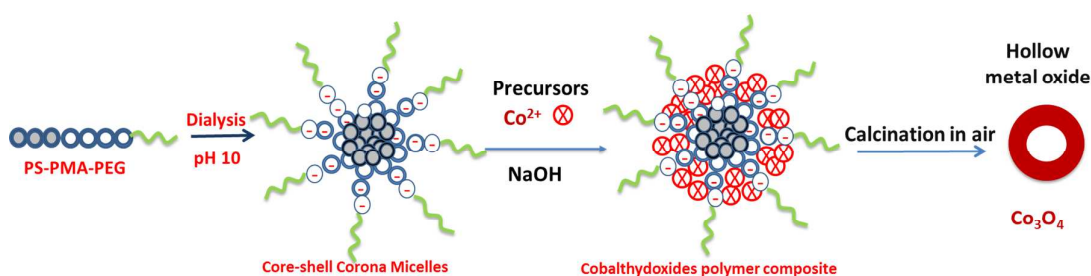
Scheme 1. Synthesis of cobalt oxide (Co_3O_4) hollow nanospheres

Experimental

Synthesis of PS-PMA-PEG

Triblock copolymer (PS-PMA-PEG) was synthesized as follows: Distilled methacrylic acid (8.02 g, 93.1 mmol), poly(ethylene glycol) methylether (4-cyano-4-pentanoate dodecyl trithiocarbonate) purchased from Aldrich (number-average molecular weight (M_n): 2,400 g/mol, 1.50 g, 0.621 mmol) and recrystallized 2,2-azobisisobutyronitrile (AIBN, 40.8 mg, 0.249 mmol) were dissolved in distilled 1,4-dioxane (62 mL). The solution was deoxygenated by Argon gas for 30 min. Polymerization was carried out at 60 °C for 8 h. The polymerization mixture was dialyzed against methanol for two days. The diblock copolymer (PEG-PMA) was recovered by evaporation. The polymer ethanol solution was poured into the large excess of n-hexane as a poor solvent (5.85 g, 61.5 %). The degrees of polymerization (DPs) for the PEG and PMA blocks were 46 and 122 estimated from 1H NMR (Figure S1). M_n and molecular weight distribution (M_w/M_n) were 1.37×10^4 g/mol and 1.39×10^4 g/mol (Figure S2), respectively, estimated from gel-permeation

chromatography (GPC). Distilled styrene (19.4 g, 0.186 mol), PEG-PMA (3.00 g, 0.234 mmol), AIBN (7.73 mg, 0.0471 mmol) were dissolved in distilled N,N-dimethylformamide (DMF, 18.6 mL). The solution was deoxygenated by Argon gas for 30 min. Polymerization was carried out at 60 ℃ for 24 h. The reaction mixture was dialyzed against tetrahydrofuran for two days. After dialysis, the solution was poured into a large excess of ethyl acetate to obtain triblock copolymer (PS-PMA-PEG, 2.07 g). M_n of the triblock copolymer and DP of the PS block were 2.67×10^4 g/mol and 132, respectively, estimated from ^{1}H NMR (Figure S3). GPC measurements for PS-PMA-PEG cannot be performed due to low solubility for the eluent.

Preparation of PS-PMA-PEG micelle

The micelle was prepared by dialysis of the DMF solution of the triblock copolymer against water. First, 0.1 g of PS-PMA-PEG was dissolved in 4.5 g of DMF under vigorous stirring for 2h. Then, 0.5 g of water was added drop by drop to the solution and the solution was kept stirring for another 2h. The mixture was dialyzed against water for three days to obtain micelle.

Fabrication of cobalt oxide hollow nanospheres

Hollow cobalt oxide nanospheres were synthesized at room temperature according to a procedure in Scheme 1. First, 1 mL of cobalt sulfate precursor solution (1.9 g mL^{-1}) was added to 10 mL of the polymeric micelle solution (0.5 mg mL^{-1}) under vigorous stirring. Subsequently, the precipitation reaction was completed by adding dilute 0.1 M NaOH solution slowly. The color of the polymeric micelle solution changed slightly from pink to colorless and to blue. In order to accelerate the reaction and to obtain the nano-crystalline structure, the solution was aged at static condition in the oven at 50 ℃ for one day. The composite particles were washed with distilled water and ethanol followed by drying in the oven at 50 ℃ for one day. Eventually, the hollow cobalt oxide nanospheres were obtained after removing the template polymer by calcination at 450 ℃ for 4 hours in air.

Characterization of PS-PMA-PEG, polymeric micelle and cobalt oxide hollow nanoparticle

^{1}H NMR spectra were obtained with a Bruker DRX-500 spectrometer. GPC analysis for PEG-PMA was performed using a refractive index detector equipped with a Shodex GF-7M HQ

column at 40 °C under a flow rate of 0.6 mL/min. A phosphate buffer (pH 9) containing 10 vol % acetonitrile was used as eluent. The values of M_n and M_w/M_n were calibrated with standard sodium poly(styrenesulfonate) samples. Dynamic light scattering (DLS) measurements were carried out with Otsuka ELS-Z Zeta potential & Particle size analyzer. Transmission electron microscope (TEM) images were obtained by using a JEOL JEM-1210 electron microscope at an accelerating voltage of 100 kV. FTIR spectra were recorded on a Bruker Vertex 70-S spectrometer. XRD patterns were obtained by Shimadzu XRD 610D X-ray Diffractometer Lab X.

**Measurements of electrochemical properties**

The electrochemical properties of cobalt oxide hollow nanosphere were examined in lithium coin cell. CR2032 type coin cells were assembled. Lithium foil was used as the anode and polypropylene as separator. For the fabrication of working electrodes, 5 mg active material together with 5 mg conducting binder (Teflon: Acetylene black = 1:2) was mixed and pressed on the stainless steel mesh under a pressure of 500 kg cm^{-2}. The as-prepared electrodes were dehydrated at 180 °C for 6 h under vacuum. The electrolyte used was 1 M lithium phosphorous hexafluoride (LiPF$_6$) in a mixture of ethylene carbonate (EC) and dimethyl carbonate (DMC) with volume ratio of 1:2 (Ube Chemicals Co. Ltd.). The cells were assembled in a glove box filled with pure argon gas. The galvanostatic charge–discharge tests of the coin cell were performed at the constant current density of 100 mA g^{-1} between 2.5-0.05 V at 30 °C. Cyclic voltammetry (CV) measurements were carried out with an HSV-100 (Hokuto Denko Inc.) over the potential range of 0.05-2.5 V vs. Li/Li$^+$ at a scanning rate of 0.1 mV s^{-1}.

Results and discussions

Figure 1a illustrates DLS histogram of PS-PMA-PEG micelles. It shows a narrow distribution of hydrodynamic diameter of 78 ± 3 nm. Figure 1b represents a TEM picture of PS-PMA-PEG micelles stained with phosphotungstic acid. As the PMA and PEO blocks are stained, the white spheres correspond to the PS core. It shows that the PS core of the template micelles have a spherical shape with mono-dispersed size, it is consistent with the PDI of the polymer solution (PDI = 0.07). The average size of the PS core is around 30 ± 2 nm.

Figure 2 shows TEM images of cobalt hollow oxide nanospheres at different magnifications. The hollow nanospheres have spherical shape with narrow size distribution. Average outer diameter of the hollow nanospheres is about ca. 60 ± 3 nm and average inner diameter is about ca. 30 ± 2 nm. The average inner diameter (ca. 30 ± 2 nm) is in consistent with the size of the PS core (ca. 30 ± 2 nm) of the template micelle. To the best of our knowledge, the obtained cobalt oxide hollow nanospheres have the smallest diameter among those nanospheres which have ever been reported.

Removal of the template micelles was checked by FTIR measurement (Figure 3). Before calcinations, there are lots of prominent absorption peaks originated from the template polymer (black and dashed line). The peak at 3000 cm^{-1} characterizes C-H stretching of aromatic group of polystyrene. The bands ranging from 1450 cm^{-1} to 1700 cm^{-1} exhibit the C=O stretching of carboxylic group. Those peaks disappeared in the spectrum of the post-calcined Co_3O_4 (red and solid line). The peaks at 670 and 692 cm^{-1} express the cobalt oxide. These facts indicate that the template polymer is completely removed by calcinations.
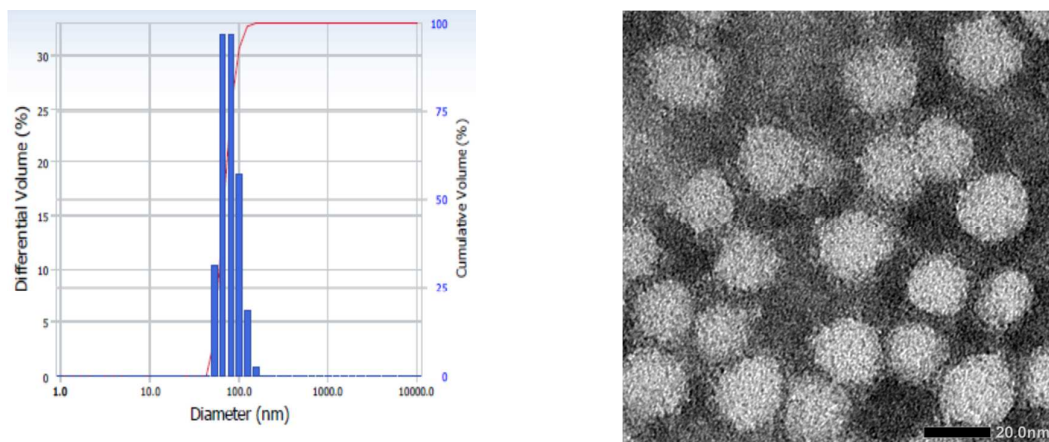

Figure 1. (a) DLS histogram of the polymeric micelles of PS-PMA-PEG and (b) TEM picture of the polymer micelles stained with 1 % phosphotungstic acid. In TEM measurements, we dropped 5 μl of the mixed solution of the micelle and phosphotungstic acid on the copper grid and dried it in the oven at 50 °C.
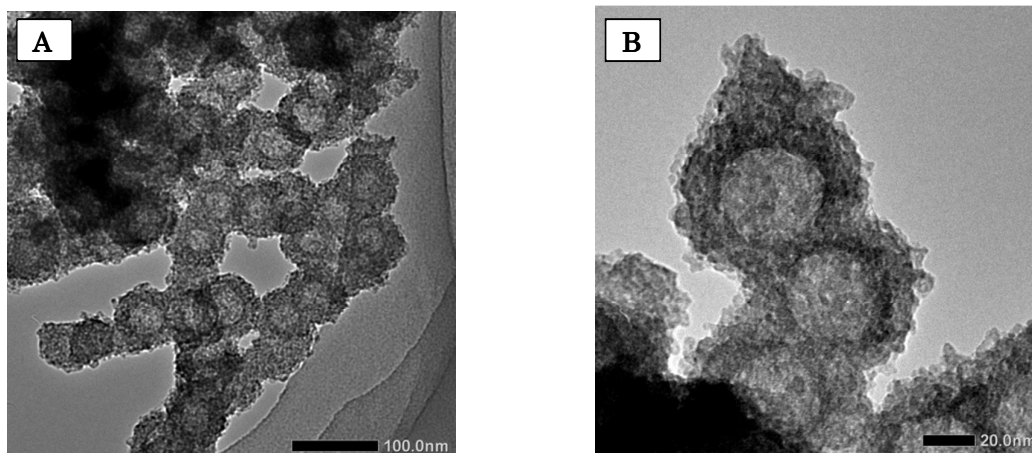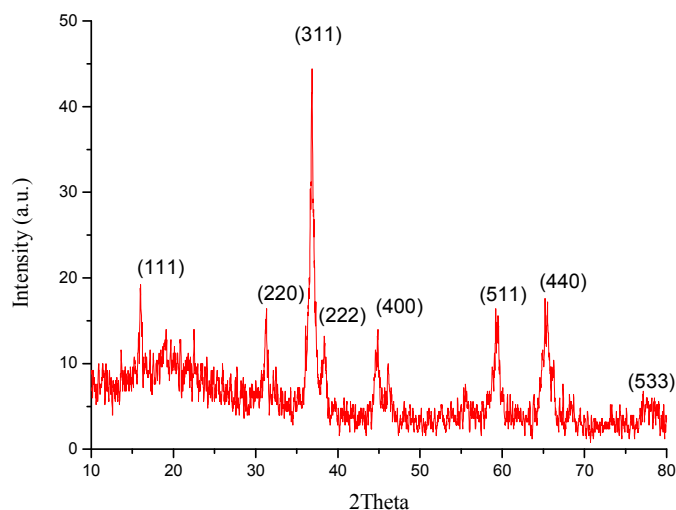
Figure 2. TEM pictures of cobalt oxide (Co_3O_4) hollow nanospheres:
(a) low magnification and (b) high magnification.
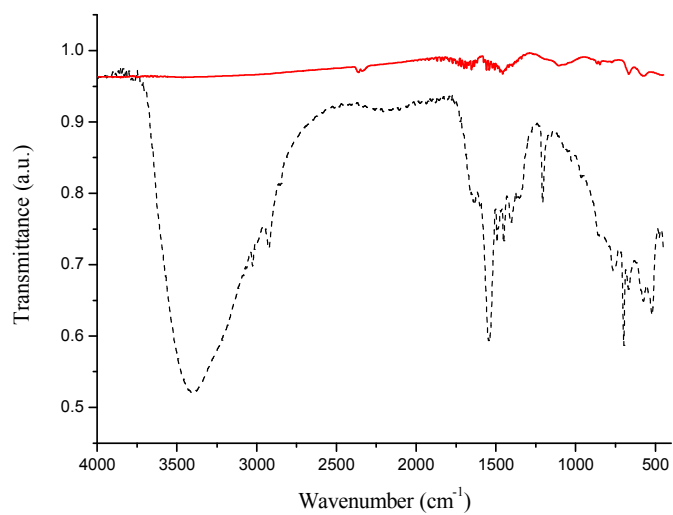
Figure 3. FTIR spectra of polymer-Co composite particles before (dashed line) and after (solid line) calcination.

Figure 4. XRD pattern of cobalt oxide hollow nanospheres

Crystal structure of the cobalt oxide hollow nanospheres was characterized by XRD. Figure 4 shows the XRD pattern of cobalt oxide hollow nanospheres calcined at 450 °C. These peaks (2θ) at 19°, 31.3°, 36.87°, 44.83°, 59.2°, and 65.2° in Fig. 4 match the JCPDS card No: 073-1701 file. This fact indicates that Co_3O_4 has the cubic structure.[25] The XRD pattern also shows that there are no characteristic peaks arising from impurities.
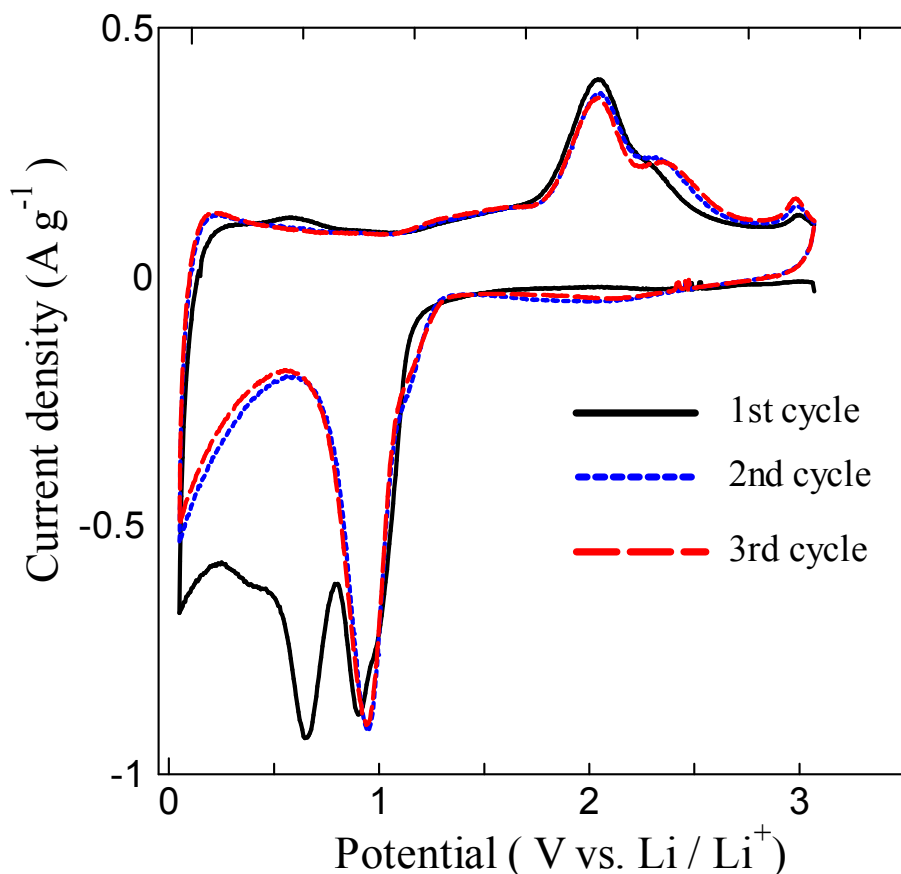
Figure 5. The cyclic voltammetry (CV) profile of Co_3O_4 hollow nanospheres

The cyclic voltammetry (CV) of Co_3O_4 nanospheres was performed for the initial three cycles in the voltage range of 0.05-2.5 V at a scan rate of 0.1 mV s^{-1}. As shown in Figure 5, two prominent cathode peaks can be observed at around 0.90 V and 0.60 V. The first cathode peak at 0.90 V could be ascribed to the reduction of Co_3O_4 into CoO and Li_2O. The second cathode peak at 0.60V for Co_3O_4 would correspond to the further reduction of CoO into Co and Li_2O and the formation of the solid electrolyte interphase (SEI) layer[26]. Similar observations have been reported in the previous papers for Co_3O_4 nanospheres.[27-28] The observed anodic peak at 2.07 V for Co_3O_4 nanospheres can be attributed to the reversible oxidation of Co to cobalt oxide. The corresponding reaction at the initial cycle can be presented as follows:

$$Co_3O_4 + 8Li^+ + 8e^- \leftrightarrow 4Li_2O + 3Co$$
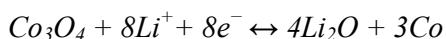
In the following cycles, the cathode peak slightly shifts to 0.95 V, while the anodic peak

remains stable. Furthermore, one can notice that the CV curves overlapped in the following cycles, revealing the good electrochemical reversibility of the Co_3O_4 electrode during the lithiation/delithiation processes.
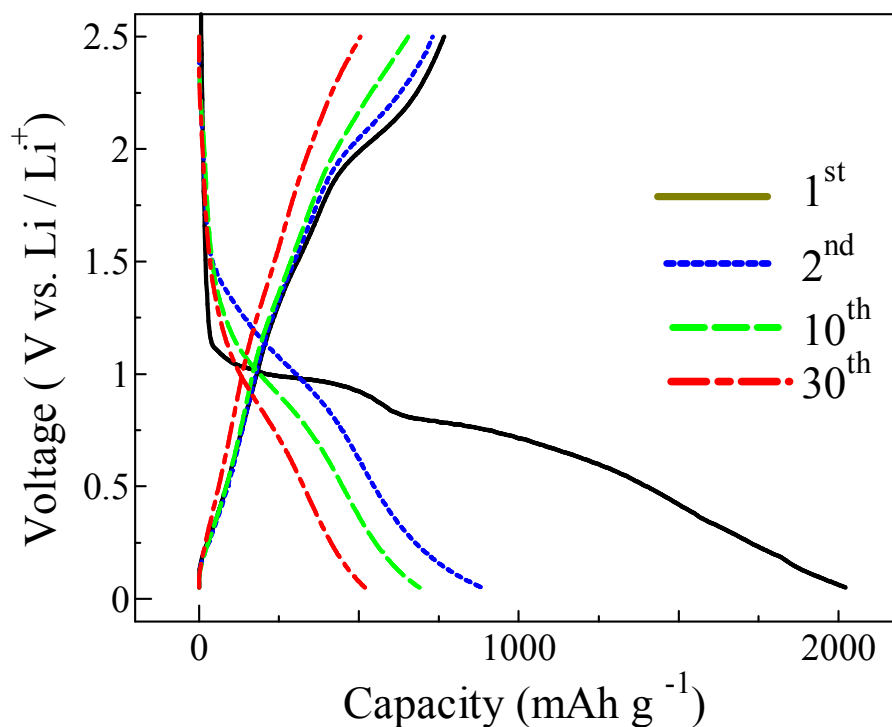
Figure 6. The charge-discharge curves of the Co_3O_4 hollow nanoparticle electrode

Figure 6 shows the charge-discharge curves of the Co_3O_4 electrode for the 1st, 2nd, 10th and 30th cycles at the current density of 100 mA g^{-1}. In the first discharge curve, there are two voltage plateaus at around 1.0 V and 0.65 V. The discharge curve turned to a sloping curve down to the cutoff volt-age of 0.05 V. The above change in the discharge curve is ascribed to the reduction of Co_3O_4 to Co metal.[29-30] These observations are consistent with the CV results as described above. The initial discharge and charge capacities are found to be 2021 mAhg[-1] and 766 mAhg[-1] respectively. The first cycle capacity loss has been observed for Co_3O_4 anode materials, which can be mainly attributed to the possible irreversible reaction such as electrolyte decomposition and formation of a SEI layer during the initial discharge process. Although the huge irreversible capacity loss was observed in the initial cycle, the Co_3O_4 electrode can still deliver a high charge capacity. The reversible specific

charge and discharge capacity of the second cycle slightly decreased to 730 and 884 mAh.g^{-1}, respectively, which shows relatively good reversibility of the Co_3O_4 electrode. Such capacity fade with cycles is normal for metal oxide conversion electrode, which is mainly caused by the pulverization of electrode materials upon cycling. Therefore, despite of the slight capacity fade upon cycling, Co_3O_4 electrode still shows a reversible capacity over 500 mAh.g^{-1} after 30 cycles. Moreover, it was found that Coulomb efficiency of Co_3O_4 electrode stabilizes at above 97% at 30th cycle.

Conclusion

The cobalt oxide hollow nanospheres have been successfully synthesized by templating *core-shell-corona* micelle of PS-PMA-PEG in aqueous solutions. The obtained hollow nanospheres were characterized by various techniques including TEM and FTIR measurements. It was shown that the hollow nanospheres have average outer diameter of about ca. 60 ± 3 nm and average inner diameter of about ca. 30 ± 2 nm. The cyclic volumetric profile proves the good electrochemical reversibility of Co_3O_4 hollow nanospheres, promising a potential application to lithium ion battery.   In future study, we plan to examine magnetic properties of the cobalt oxide hollow nanospheres to elucidate the effect of hollow structure on the magnetic properties.

Acknowledgement

References

1   X. Wang, W. Tian, T. Zhai, C. Zhi, Y. Bando and D. Golberg, *J. Mater. Chem.,* 2012, **22**, 23310–23326.

2   D. Wang, Y. Yu, H. He, J. Wang, W. Zhou, Abruna, Hector D., *ACS Nano,* 2015, **9**, 1775-1781.

3   Q. Ye, H. Yoshikawa and K. Awaga, *Material,* 2010, **3**, 1244-1268.

4   J. Hu, Min Chen, X. Fang and L. Wu, *Chem. Soc. Rev.*, 2011, **40**, 5472–5491.

5   J. Jiang and L. C. Li, *Matter. Lett.,* 2007, **6***,* 4894-4896.

6   S. Y. Lian, E. B. Wang, L. Gao, and L. Xu, *Matter. Lett.,* 2006, **61**, 3893-3896.

7   X. H. Liu, G. Z. Qiu, and X. G. Li, *Nanotechnology,* 2005, **16**, 3035-3040.

8   T. He, D. R. Chen, X. L. Jiao, Y. Xu and Y. X. Gu, *Langmuir,* 2004, **20**, 8404-8408.

9   Y. C. Chen, Y. G. Zhang and S. Q. Fu, *Mater. Lett.,* 2007, **61**, 701-705.

10   M. Sasidharan and K. Nakashima, *Mater. Lett.,* 2012, **73**, 4-7.

11   C. S. Cheng, M. Serizawa, H. Sakata, and T. Hirayama, *Matter. Chem. Phys.*, 1998, **53**, 225

12   M. Ando, T. Kobayashi, S Iijima, and M. Haruta, *J. Mater. Chem.*, **1997**, 7, 1779

13   T. Maruyama and S. Arai, *J. Electrochem. Soc,* 1996, **143**,1383 ()

14   G. X. Wang, Y. Chen, K. Konstantinov, J. Yao, J. H. Ahn, H. K. Liu, and S. X. Dou, *J. Alloys Compd.* 340, 2002, L5

15   E. Papisa, R. Gornatia, *Toxicology Letters,* 2009, **189**, 253–259

16   M. Sasidhara and K. Nakashima, *Acc. Chem. Res.*, 2014, **47**, 157-167.

17   B. P. Bastakoti, K. C. W. Wu, M. Inoue, S. Yusa, K. Nakashima, and Y. Yamauchi, *Chem. Eur. J.,* 2013*,* **19**, 4812 – 4817.

18   A. Khanal, Y. Inoue, M. Yada and K. Nakashima, *J. Am. Chem. Soc*., 2007, **129**, 1534-1534.

19   M. Sasidharan and K. Nakashima, *Chem. Commun.,* 2011, **47**, 6921-6923.

20   M. Sasidharan and K. Nakashima*, Ionics*, 2013, **19**, 25-31.

21   M. Sasidharan, N. Gunawardhana, M. Inoue, S. Yusa, M.Yoshio and K. Nakashima, *Chem. Commum*., 2012, **48**, 3200-3202.

22   M. Alam, W. Zhao, S. Zhai, S. Yusa, H. Noguchi and K. Nakashima, *Chem. Lett.,* 2014, **43**, 1426-1428.

23   S. Zhai, S. Yusa and K. Nakashima, *Bull. Chem. Soc. Jpn*, 2013, **86**, 884-890.

24   M. Alam, K. Hashimoto, C. Yamaguchi, S. Yusa and K. Nakashima, *Bull. Chem. Soc. Jpn*, in press.

25   H. Liang, J. M. Raitano, L. Zhang and S. Chan, *Chem. Commun.,* 2009, **458**, 746–749

26   D. Larcher, G. Sudant, J. B. Leriche, Y. Chabre and J. M. Tarascon, *J. Electrochem. Soc.*, 2002, **149**, A234-A241.

27   G. Zhou, L. Li, Q. Zhang, N. Li and F. Li, *J. Power Sources,* 2011, **196**, 6987-6991.

28   X.W. Lou, D. Deng, J.Y. Lee and L.A. Archer, *J. Mater. Chem.,* 2008, **18**, 4397-4401.

29   Y. Fan, H. Shao, J. Wang, L. Liu, J. Zhang and C. Cao, *Chem. Commun.,* 2011, **47**, 3469-3471.

30   L. Zhan, S. Wang, L. X. Ding, Z. Li and H. Wang, *Electrochimica Acta.,* 2014, **135***,* 35-41.